High-fidelity base editor with no detectable genome-wide off-target effects

Erwei Zuo[1,2,†,*], Yidi Sun[3,4,†], Tanglong Yuan[1,†], Bingbing He[2,†], Changyang Zhou[2,†], Wenqin Ying[2], Jing Liu[1], Wu Wei[4,5], Rong Zeng[3,6], Yixue Li[4,6,7,8,9,*], Hui Yang[2,*,10]

[1]Center for Animal Genomics, Agricultural Genome Institute at Shenzhen, Chinese Academy of Agricultural Sciences, Shenzhen 518124, China
[2]Institute of Neuroscience, State Key Laboratory of Neuroscience, Key Laboratory of Primate Neurobiology, CAS Center for Excellence in Brain Science and Intelligence Technology, Shanghai Research Center for Brain Science and Brain-Inspired Intelligence, Shanghai Institutes for Biological Sciences, Chinese Academy of Sciences, Shanghai 200031, China
[3]CAS Key Laboratory of Systems Biology, CAS Center for Excellence in Molecular Cell Science, Institute of Biochemistry and Cell Biology, Shanghai Institutes for Biological Sciences, Chinese Academy of Sciences, University of Chinese Academy of Sciences, Shanghai, 200031, China
[4]Bio-Med Big Data Center, Key Laboratory of Computational Biology, CAS-MPG Partner Institute for Computational Biology, Shanghai Institute of Nutrition and Health, Shanghai Institutes for Biological Sciences, University of Chinese Academy of Sciences, Chinese Academy of Sciences Shanghai, 200031, China
[5]Center for Biomedical Informatics, Shanghai Children's Hospital, Shanghai Jiao Tong University, Shanghai 200040, China
[6]Department of Life Sciences, Shanghai Tech University, 100 Haike Road, Shanghai, 200031, China
[7]School of Life Sciences and Biotechnology, Shanghai Jiao Tong University, Shanghai, 200240, China.
[8]Collaborative Innovation Center for Genetics and Development, Fudan University, Shanghai, China.
[9]Shanghai Center for Bioinformation Technology, Shanghai Academy of Science & Technology, Shanghai, China
[10]Lead contact
†These authors contributed equally to this work.
*Corresponding authors. E-mail: erweizuo@163.com, yxli@sibs.ac.cn or huiyang@ion.ac.cn

Base editors hold promise for correcting pathogenic mutations, while substantial single nucleotide variations (SNVs) on both DNA and RNA were generated by cytosine base editors (CBEs). Here we examined possibilities to reduce off-target effects by engineering cytosine deaminases. By screening 24 CBEs harboring various rAPOBEC1 (BE3) or human APOBEC3A (BE3-hA3A) mutations on the ssDNA or RNA binding domain, we found 8 CBE variations could maintain high on-target editing efficiency. Using Genome-wide Off-target analysis by Two-cell embryo Injection (GOTI) method and RNA sequencing analysis, we found DNA off-target SNVs induced by BE3 could be completely eliminated in BE3^{R126E} but the off-target RNA SNVs was only slightly reduced. By contrast, BE3-hA3A^{Y130F} abolished the RNA off-target effects while could not reduce the DNA off-target effects. Notably, BE3^{R132E}, BE3$^{W90Y+R126E}$ and BE3$^{W90F+R126E}$ achieved the elimination of off-target SNVs on both DNA and RNA, suggesting the feasibility of engineering base editors for high fidelity deaminases.

Base editors have been widely applied to perform targeted base editing and hold great potential for correcting pathogenetic mutations[1]. However, previous studies have identified off-target DNA edits by cytosine base editors (CBEs)[2, 3], the most widely used cytosine base editors with rat APOBEC1 (rAPOBEC1) enzyme[4, 5]. Recently, several groups reported that CBEs with rAPOBEC1 (BE3) or human APOBEC3A (BE3-hA3A) can cause extensive transcriptome-wide RNA off-target edits in human cells[6-8]. These off-target RNA SNVs could be substantially decreased by screening CBEs harboring various rAPOBEC1 or hA3A mutations, but the DNA off-target edits of these variants were unknown[6-8] .

The observation of unwanted DNA and RNA off-target effects both have important implications for research and therapeutic applications of these technologies. Previous studies only examined the DNA (Zuo et al., 2019) or RNA off-target effects (Zhou et al., 2019) of base editors, here we analyzed both the DNA and RNA off-target effects of multiple engineered CBE variants by Genome-wide Off-target analysis by Two-cell embryo Injection (GOTI) and RNA-Seq analysis. We found that some variants could eliminate the DNA off-target activity while sustained RNA off-target effects. Conversely, some variant abolished the RNA off-target effects while maintained the DNA off-targets. Importantly, we successfully obtained three variants with the elimination of both DNA and RNA off-target effects.

We introduced various point mutations into rAPOBEC1 affecting the DNA[9-14] or RNA[14, 15] editing activity suggested by previous studies (Fig. 1a). The variants included deletions and mutations at the L-enriched 5' or 3' terminals of APOBEC1 (Del32, R33A, K34A, Del34, Del77, Del116, Del169, Del182, P190A and P191A), point mutations on the putative catalytic active site of APOBEC1 (H61A, H61R, V62A, E63A, E63Q, C93S, C96S). Based on the structure of human APOBEC3G[10,

[11], R126 is predicted to have interaction with the phosphate backbone of ssDNA (corresponding to R320 in APOBEC3G) (Fig. 1b, c). Compared with other mutations, R126E maintained on-target editing activity[9]. R128 and R132[9] are near to R126 and could also affect the accessibility of ssDNA, so we also introduced mutations of R128E and R132E (Fig. 1a-c). We also examined the effect of combination of point mutations in the domain responsible for the hydrophobicity of the active site on APOBEC1 (W90A, W90F, W90Y), which was reported to narrow the width of base-editing window[9, 10].

We transfected HEK293T cells with plasmids encoding BE3 base editors harboring various mutations and evaluated their effects on both on-target efficiency and off-target rate. We tested the on-target activity of these variants on 10 genomic loci. Totally, by screening 23 engineered BE3 variants, we found 7 variants (R33A, K34A, V62A, W90F+R126E, W90Y+R126E, R126E and R132E) remained the on-target efficiency, and 4 of them (W90F+R126E, W90Y+R126E, R126E, R132E) showed no increase of indel rates (Fig. 1d and Supplementary Table 1). Besides, all of them showed no significantly difference on the editing window widths (Supplementary Fig. 1). Alternatively, we also tested one variant on hA3A (BE3-hA3A^{Y130F}), reported to have high DNA on-target efficiency[16, 17], and found it remained high on-target editing activities (Fig. 1d).

We next performed GOTI to evaluate the DNA off-target edits of the variants with high DNA on-target efficiency (BE3^{R126E}, BE3^{R132E}, BE3$^{W90Y+R126E}$, BE3$^{W90F+R126E}$ and BE3-hA3A^{Y130F}) (Supplementary Table 2). The embryonic development was not affected by these variants injection except for BE3-hA3A (Supplementary Fig. 2). The on-target efficiency of these variants were confirmed by whole-genome sequencing (Fig. 2a). Notably, the number of DNA off-target SNVs in the embryos treated with BE3^{R126E}, BE3^{R132E}, BE3$^{W90Y+R126E}$ or BE3$^{W90F+R126E}$ was significantly reduced from 283 +/- 32 in wild-type BE3-treated embryos to 28 +/- 6 for BE3^{R126E}, 43 +/- 11 for BE3^{R132E}, 12 +/- 3 for BE3$^{W90Y+R126E}$ and 39 +/- 27 for BE3$^{W90F+R126E}$, similar to that found in non-edited control embryos (14 SNVs on average) and close to that of spontaneous mutation (Fig. 2b, Supplementary Fig. 3 and Supplementary Table 3). Besides, we observed no mutation bias and no SNVs that overlapped with the predicted off-target sites (Fig. 2c and Supplementary Fig. 4), suggesting the absence of DNA off-target SNVs induced by these variants. However, the BE3-hA3A^{Y130F} variant still generated substantial DNA off-target SNVs (409 +/- 86) (Fig. 2b and 2c).

Moreover, we also evaluated the potential off-target effects on transcriptome of these variants. We found evident decrease of RNA off-target SNVs in BE3^{R126E}, but the number was still significantly higher than that of the control group transfected with GFP (Fig. 3a and 3b). Intriguingly, two variants BE3^{R132E} and BE3$^{W90F+R126E}$ (also know as BE3-FE1) [9] showed complete elimination of the RNA off-target edits. Combined with our previous results that BE3$^{W90Y+R126E}$ (also know as BE3-YE1) [9]

could completely eliminated the RNA off-target edits (Fig. 3a and 3b), we here obtained three variants, BE3^{R132E}, BE3$^{W90Y+R126E}$ and BE3$^{W90F+R126E}$, with complete abolish of both DNA and RNA off-target effects.

Considering that GOTI was developed to examine the sgRNA-independent off-target effects, we also examined the sgRNA-dependent off-target sites as previous studies[18]. We found no increase of the number of these sgRNA-dependent off-targets in all the variants (Supplementary Fig. 5).

In summary, by screening dozens of mutations on rAPOBEC1 or hA3A from multiple researches before, we found three variants with complete abolish of both DNA and RNA off-targets with no compromise for on-target activity. Although BE3^{R132E}, BE3$^{W90Y+R126E}$ and BE3$^{W90F+R126E}$ have been reported to remain editing efficiencies as BE3[9], off-target evaluation is necessary for their clinical application. In addition, we found that BE3^{R126E} could eliminate the DNA off-target effects but not the RNA off-targets, while BE3-hA3A^{Y130F} only reduced the RNA off-target effects, indicating that the elimination of DNA off-target effects was not eligible for the minimization of RNA off-target effects, and vice versa. Engineered variants with high fidelity on both DNA and RNA provide a safe tool for gene editing. Notably, the study described here demonstrates that the DNA and RNA off-target effects of BE3 could be simultaneously eliminated by engineering APOBEC1 with mutations on the putative ssDNA binding domain and hydrophobic domain but not on catalytic domain. Therefore, our work illustrates how the off-target effects can be defined and minimized for research and therapeutic applications (Fig. 3c). This approach for fusion protein optimization could be generalized in other synthetic tools such as CRISPR/Cas9 derivates (Supplementary Fig. 6).

Acknowledgments

We thank FACS facility HW, LQ, SQ in ION and MZ in IPS, LY in Big Data Platform (SIBS,CAS). These work were supported by R&D Program of China (2018YFC2000100 and 2017YFC1001302), CAS Strategic Priority Research Program (XDB32060000), National Natural Science Foundation of China (31871502, 31522037, 31822035), Shanghai Municipal Science and Technology Major Project (2018SHZDZX05), Shanghai City Committee of science and technology project (18411953700, 18JC1410100), National Science and Technology Major Project (2015ZX10004801-005), National Key Research and Development Program of China (2017YFA0505500, 2016YFC0901704) and the Agricultural Science and Technology Innovation Program.

Author contributions

EZ designed and performed experiments. YS, WW, RZ and LY performed data analysis. TY, BH and JL performed PCR analysis. WY performed mouse embryo transfer. HY and YL supervised the project and designed experiments. YS and HY

wrote the paper.

Competing financial interests

The authors declare no competing financial interests.

Data and materials availability

All the sequencing data were deposited in NCBI Sequence Read Archive (SRA) under project accession PRJNA527003.

REFERENCES

1. Rees, H.A. & Liu, D.R. Base editing: precision chemistry on the genome and transcriptome of living cells. *Nat Rev Genet* (2018).
2. Zuo, E. et al. Cytosine base editor generates substantial off-target single nucleotide variants in mouse embryos. *Science*, published online (2019).
3. Jin, S. et al. Cytosine, but not adenine, base editors induce genome-wide off-target mutations in rice. *Science* , published online (2019).
4. Komor, A.C., Kim, Y.B., Packer, M.S., Zuris, J.A. & Liu, D.R. Programmable editing of a target base in genomic DNA without double-stranded DNA cleavage. *Nature* **533**, 420-+ (2016).
5. Rees, H.A. & Liu, D.R. Base editing: precision chemistry on the genome and transcriptome of living cells. *Nat Rev Genet* **19**, 770-788 (2018).
6. Grunewald, J. et al. Transcriptome-wide off-target RNA editing induced by CRISPR-guided DNA base editors. *Nature* **569**, 433-437 (2019).
7. Grünewald, J. et al. CRISPR adenine and cytosine base editors with reduced RNA off-target activities. 631721 (2019).
8. Zhou, C. et al. Off-target RNA mutation induced by DNA base editing and its elimination by mutagenesis. *Nature* (2019).
9. Kim, Y.B. et al. Increasing the genome-targeting scope and precision of base editing with engineered Cas9-cytidine deaminase fusions. *Nat Biotechnol* **35**, 371-376 (2017).
10. Holden, L.G. et al. Crystal structure of the anti-viral APOBEC3G catalytic domain and functional implications. *Nature* **456**, 121-124 (2008).
11. Chen, K.M. et al. Structure of the DNA deaminase domain of the HIV-1 restriction factor APOBEC3G. *Nature* **452**, 116-119 (2008).
12. Petersen-Mahrt, S.K. & Neuberger, M.S. In vitro deamination of cytosine to uracil in single-stranded DNA by apolipoprotein B editing complex catalytic subunit 1 (APOBEC1). *J Biol Chem* **278**, 19583-19586 (2003).
13. Harris, R.S., Petersen-Mahrt, S.K. & Neuberger, M.S. RNA editing enzyme APOBEC1 and some of its homologs can act as DNA mutators. *Mol Cell* **10**, 1247-1253 (2002).
14. Teng, B.B. et al. Mutational analysis of apolipoprotein B mRNA editing enzyme (APOBEC1). structure-function relationships of RNA editing and dimerization. *J Lipid Res* **40**, 623-635 (1999).
15. Teng, B., Burant, C.F. & Davidson, N.O. Molecular cloning of an apolipoprotein B messenger RNA editing protein. *Science* **260**, 1816-1819 (1993).
16. Wang, X. et al. Efficient base editing in methylated regions with a human APOBEC3A-Cas9 fusion. *Nat Biotechnol* **36**, 946-949 (2018).

17. Gehrke, J.M. et al. An APOBEC3A-Cas9 base editor with minimized bystander and off-target activities. *Nat Biotechnol* **36**, 977-982 (2018).

18. Gaudelli, N.M. et al. Programmable base editing of A*T to G*C in genomic DNA without DNA cleavage. *Nature* **551**, 464-471 (2017).

Figure legends

Figure 1. On-target efficiency of engineered CBEs. a The predicted structure of APOBEC1 with various rAPOBEC1 mutations. Mutated residues were highlighted and marked on the structure. **b** The sequence alignment between APOBEC3G and APOBEC1. Amino acid, identical residues; +, conservative substitutions. Green triangle represents residues in the hydrophobic active domain of APOBEC3G, and yellow stars indicate residues on the ssDNA binding domain. **c** The crystal structure of APOBEC3G. **d** The on-target efficiency and indel frequencies of different versions of engineered CBEs. Purple triangles indicate variants selected for the off-target evaluation. $n = 3$ biological replicates for each group.

Figure 2. On-target and off-target evaluation of engineered CBEs by GOTI. a On-target efficiency of BE3 and CBE variants from WGS data. **b** The comparison of the total number of detected off-target SNVs. $n = 2$ for Cre, $n = 6$ for BE3, $n = 10$ for $BE3^{R126E}$, $n = 2$ for $BE3^{R132E}$, $n = 5$ for $BE3^{W90Y+R126E}$, $n = 2$ for $BE3^{W90F+R126E}$ and $n = 3$ for BE3-hA3A^{Y130F} groups. P value was calculated by two-sided Student's t-test. $^{*}P < 0.05$, $^{**}P < 0.01$, $^{***}P<0.001$. **c** Proportion of C>T and G>A mutations for Cre, BE3, and CBE variants-treated groups.

Figure 3. RNA off -target evaluation of engineered CBEs. a The comparison of the total number of detected RNA off-target SNVs. $n = 6$ for GFP, $n = 8$ for BE3, $n = 6$ for $BE3^{R126E}$, $n = 3$ for $BE3^{R132E}$, $n = 2$ for $BE3^{W90Y+R126E}$, $n = 3$ for $BE3^{W90F+R126E}$, $n = 3$ for BE3 (hA3A) and $n = 3$ for BE3-hA3A^{Y130F} groups. P value was calculated by two-sided Student's t-test. $^{*}P < 0.05$, $^{**}P < 0.01$, $^{***}P<0.001$. **b** Proportion of C>U and G>A mutations for GFP, BE3, and BE3 variants-treated groups. **c** Model of CBE optimization. The nickase Cas9 (nCas9) of engineered CBE loses one nuclease activity of Cas9 while remains the DNA binding ability. In contrast to nCas9, mutant APOBEC1 of engineered CBE loses the binding ability of ssDNA and RNA but remains the deaminase activity. AD, active domain; BD, binding domain; APOBEC1, rAPOBEC1; UGI, uracil DNA glycosylase inhibitor.

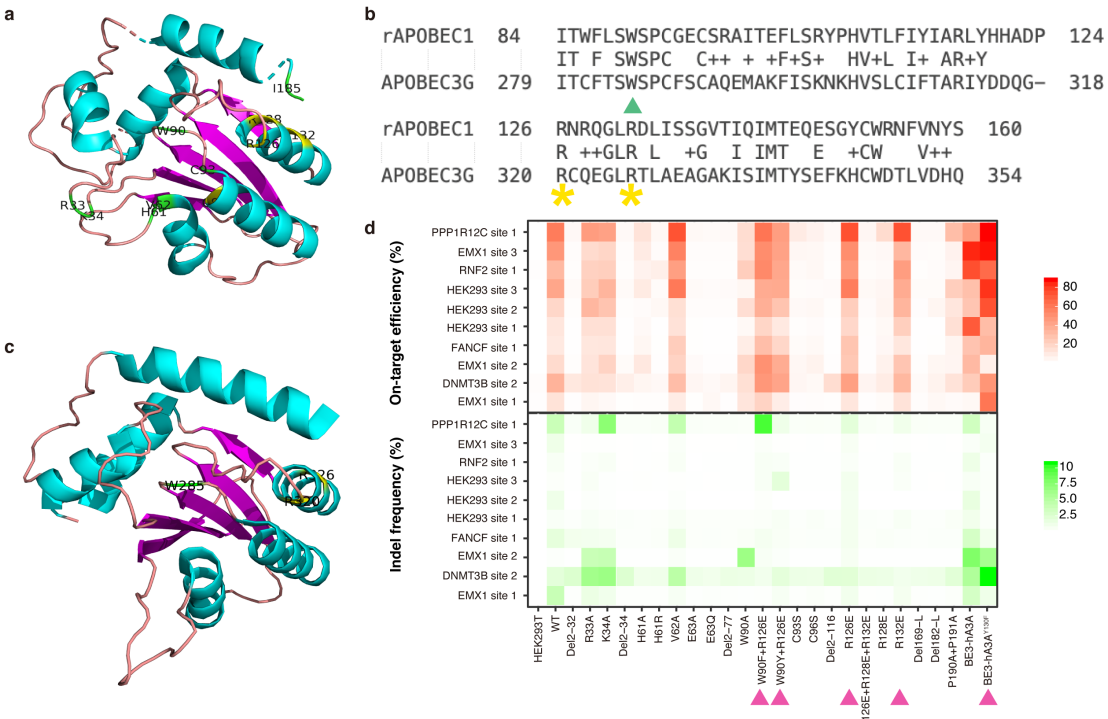

247

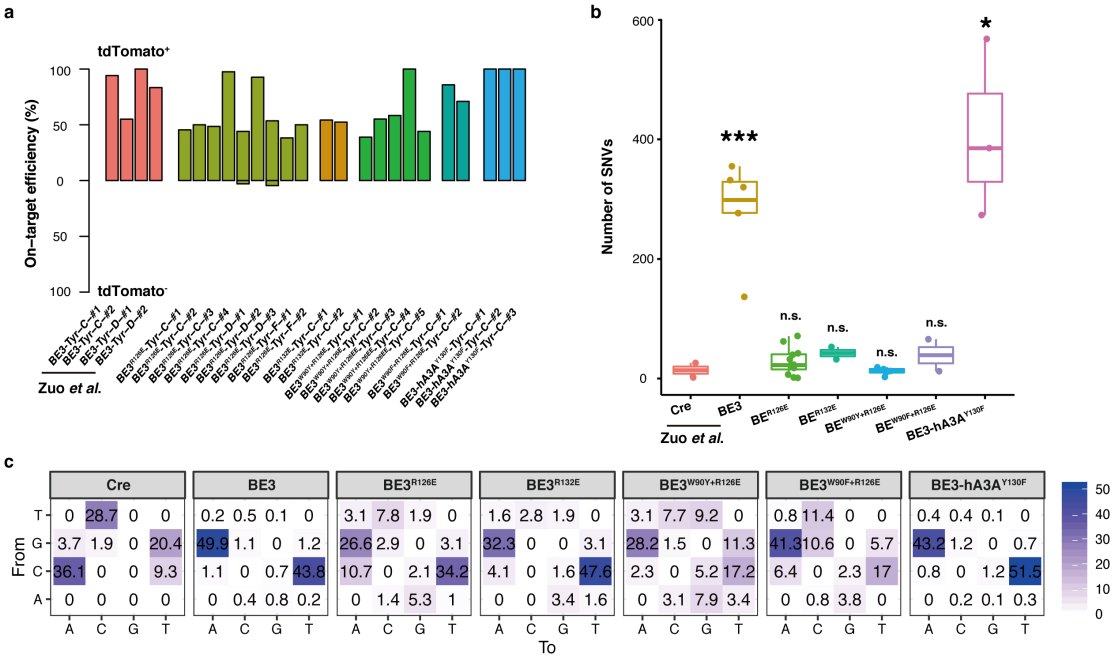

248
249

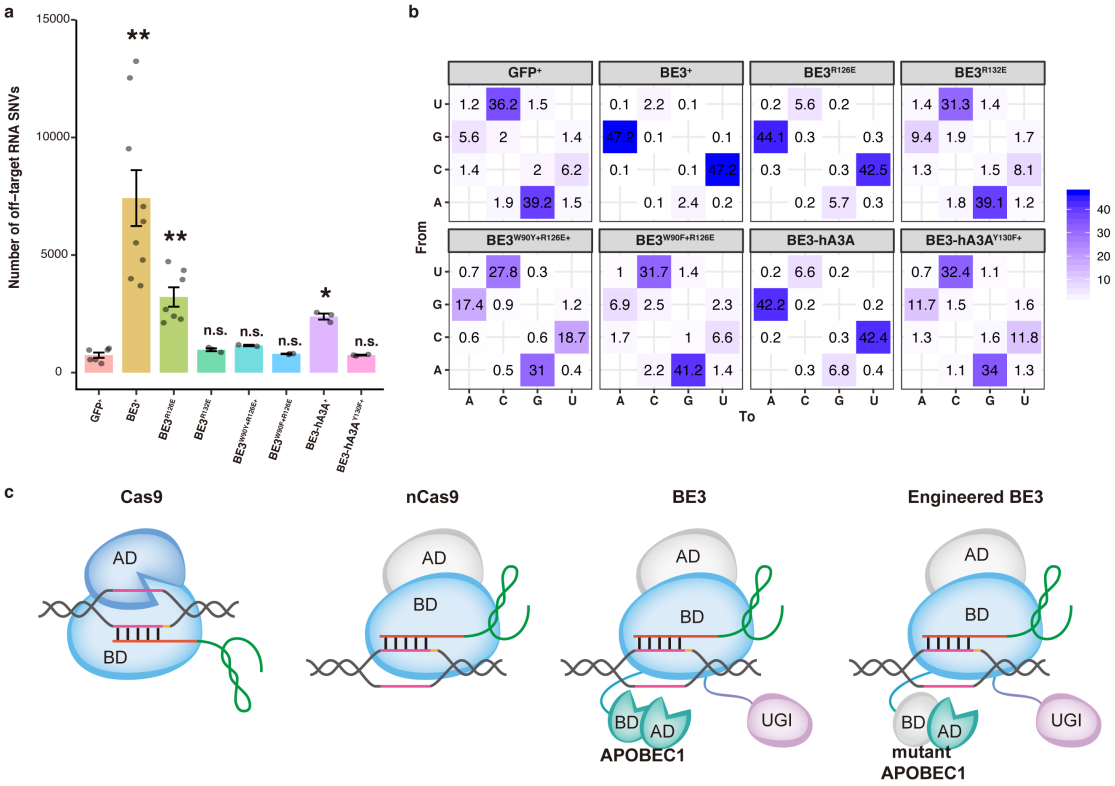

250

Supplementary Information

High-fidelity base editor with no detectable genome-wide off-target effects

Erwei Zuo[1,2,†,*], Yidi Sun[3,4,†], Tanglong Yuan[1,†], Bingbing He[2,†] , Changyang Zhou[2,†], Wenqin Ying[2], Jing Liu[1], Wu Wei[4,5], Rong Zeng[3,6], Yixue Li[4,6,7,8,9,*], Hui Yang[2,*,10]

This PDF file includes:

Materials and Methods

Animal care

Heterozygous Ai9 (full name B6.Cg-Gt (ROSA) 26Sortm9 (CAG-td-Tomato) Hze/J; JAX strain 007909) male mice and female C57BL/6 mice (4 weeks old) were mated for embryo collection. ICR females were used for recipients. The animals usage and care complied with the guideline of the Biomedical Research Ethics Committee of Shanghai Institutes for Biological Science, Chinese Academy of Sciences.

Generation of mutant base editor mRNA and sgRNA

T7 promoter was added to base editor coding region by PCR amplification of plasmid, using primer base editor F and R. T7-base editor PCR product was purified and used as the template for in vitro transcription (IVT) using mMESSAGE mMACHINE T7 ULTRA kit (Life Technologies). T7 promoter was added to sgRNA template by PCR amplification of px330. The T7-sgRNA PCR product was purified and used as the template for IVT using MEGA shortscript T7 kit (Life Technologies). T7 promoter was added to Cre template by PCR amplification. T7-Cre PCR product was purified and used as the template for *in vitro* transcription (IVT) using mMESSAGE mMACHINE T7 ULTRA kit (Life Technologies). Cas9 mRNA, Cre mRNA and sgRNAs were purified using MEGA clear kit (Life Technologies) and eluted in RNase-free water.

sgRNA sequences

Locus	Sequence (5'-3')
Tyr-C[1]	GACCTCAGTTCCCCTTCAAAGGG
Tyr-D[1]	CTGTGCCAAGGCAGAAACCCTGG
Tyr-F	TGCGGCCAGCTTTCAGGCAGAGG

Primers

Name	Sequence (5'-3')
base editor IVT F	TCCGCGGCCGCTAATACGACT
base editor IVT R	TGGTTCTTTCCGCCTCAGAAGCC
Cre IVT F	TAATACGACTCACTATAGGGAGACAGATCACCTTTC CTATCAACC
Cre IVT R	TCGGTATTTCCAGCACACTGGA
Tyr-C IVT F	TAATACGACTCACTATAGGGGACCTCAGTTCCCCTT CAAAGTTTTAGAGCTAGAAATAG
Tyr-D IVT F	TAATACGACTCACTATAGGGCTGTGCCAAGGCAGA AACCCGTTTTAGAGCTAGAAATAG
sgRNA IVT R	AAAAGCACCGACTCGGTGCC

2-cell Embryo Injection, Embryo Culturing, and Embryo Transplantation

Super ovulated C57BL/6 females (4 weeks old) were mated to heterozygous Ai9 (full name B6.Cg-Gt(ROSA)26Sortm9(CAG-td-Tomato)Hze/J; JAX strain 007909) males, and fertilized embryos were collected from oviducts 23 h post hCG injection. For 2-cell editing, the mixture of BE3 mRNA (10 or 50 ng/μl) or $BE3^{R126E}$ mRNA (50 ng/μl), sgRNA (50 ng/μl) and Cre mRNA (2 ng/μl) was injected into the cytoplasm of one blastomere of 2-cell embryo 48 h post hCG injection in a droplet of M2 medium containing 5 μg/ml cytochalasin B (CB) using a FemtoJet microinjector (Eppendorf) with constant flow settings. The injected embryos cultured in KSOM medium with amino acids at 37 °C under 5% CO_2 in air for 2 hours and then transferred into oviducts of pseudopregnant ICR females at 0.5 dpc.

Cloning

Site-directed mutagenesis of BE3 was done using NEBuilder HiFi DNA Assembly Master Mix (New England BioLabs). Briefly, a primer with an overhang containing the desired point mutation was used to amplify the appropriate vector plasmid by PCR. pCMV-BE3 variants-polyA-pCMV-mCherry-polyA was generated through NEBuilder HiFi DNA Assembly, by combining a PCR-amplified pCMV-mCherry-poly A with a digested pCMV-BE3 variants backbone. pCMV-EGFP-polyA-U6-sgRNA were generated through NEBuilder HiFi DNA Assembly, by combining a PCR-amplified U6-sgRNA with a digested pCMV-EGFP-poly A backbone.

Cell culture, transfections and FACS

HEK293T cells were maintained in Dulbecco's modified eagle medium (DMEM) supplemented with 10% fetal bovine serum (FBS) in a 37°C humidified incubator with 5% CO2. pCMV-BE3 (WT/BE3 variants)-polyA-pCMV-mCherry-polyA and pCMV-EGFP-polyA-U6-sgRNA expression plasmids were co-transfected using Lipofectamine 3000 (ThermoFisher Scientific) according to the manufacturer's protocol. 72 hr post transfection, cells were washed with phosphate buffered saline (PBS) and trypsinized using 0.05% trypsin-EDTA. Cell suspension was filtered through a 40-μm cell strainer, and EGFP/mCherry positive cells were isolated by FACS.

FACS

To isolate mouse embryonic cells, the prepared tissues were dissociated enzymatically in an incubation solution of 5 mL Trypsin-EDTA (0.05%) at 37°C for 30min. The digestion was stopped by adding 5 ml of DMEM medium with 10% Fetal Bovine Serum (FBS). Fetal tissues were then homogenized by passing 30-40 times through a 1ml pipette tips. The cell suspension was centrifuged for 6 min (800 rpm), and the pellet was resuspended in DMEM medium with 10% FBS. Finally, the cell suspension was filtered through a 40-μm cell strainer, and $tdtomato^{+}$/$tdtomato^{-}$ cells were isolated by FACS. Samples were found to be >95% pure when assessed with a second round of flow cytometry and fluorescence microscopy analysis.

Whole genome sequencing and data analysis

DNeasy blood and tissue kit (catalog number 69504, Qiagen) was used to extract genomic DNA from cells following the manufacturer's instructions. Whole genome sequencing was performed at mean coverages of 50x by Illumina HiSeq X Ten. BWA (v0.7.12) was used to map qualified sequencing reads to the reference genome (mm10). The mapped BAM files were then sorted and marked using Picard tools (v2.3.0). To identify the genome wide *de novo* SNVs with high confidence, we conducted single nucleotide variation calling on three algorithms, Mutect2 (v3.5), Lofreq (v2.1.2) and Strelka (v2.7.1), separately [2-4]. In parallel, Mutect2 (v3.5), Scalpel (v0.5.3) and Strelka (v2.7.1) were run individually for the detection of whole genome *de novo* indels [2, 4, 5]. The overlap of three algorithms of SNVs or indels were considered as the true variants. All the sequencing data were deposited in NCBI Sequence Read Archive (SRA) under project accession PRJNA527003.

Potential off-targets of targeted sites were predicted using two previous reported algorithms, Cas-OFFinder (http://www.rgenome.net/cas-offinder/) and CRISPOR (http://crispor.tefor.net/) with all possible mismatches [6, 7].
The SNVs and indels were annotated with annovar (version 2016-02-01) using RefSeq database [8].

Structure prediction

Amino acid sequences of rat APOBEC1 and human APOBEC3G were retrieved from UniProt (https://www.uniprot.org/) and sequence alignment was performed with NCBI blastp (https://blast.ncbi.nlm.nih.gov/Blast.cgi?PROGRAM=blastp&PAGE_TYPE=BlastSearch&LINK_LOC=blasthome). The structure of rAPOBEC1 was predicted by protein structure prediction server, (PS)[2] [9, 10] according to the consensus sequence and secondary structure information for proteins with known structures. The crystal structure of APOBEC3G was downloaded from PDB (http://www.rcsb.org/3d-view/3IQS) and presented using PyMOL (v2.3.2).

Statistical analysis

R version 3.5.1 (http://www.R-project.org/) was used to conduct all the statistical analyses in this work. All tests conducted were two-sided, and the significant difference was considered at $P < 0.05$.

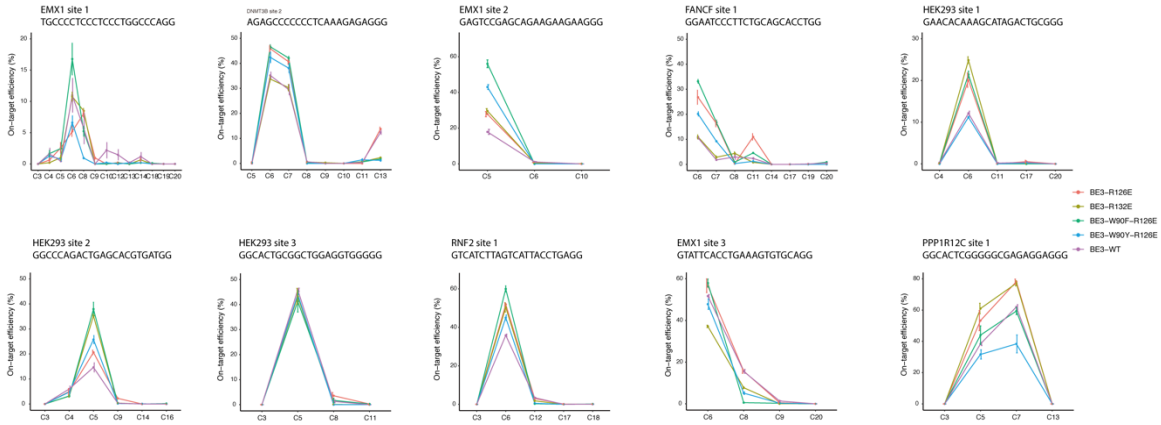

Supplementary Figure 1 The editing window of the BE3 and BE3 variants in different target sites. *n* = 3 biological replicates for each group.

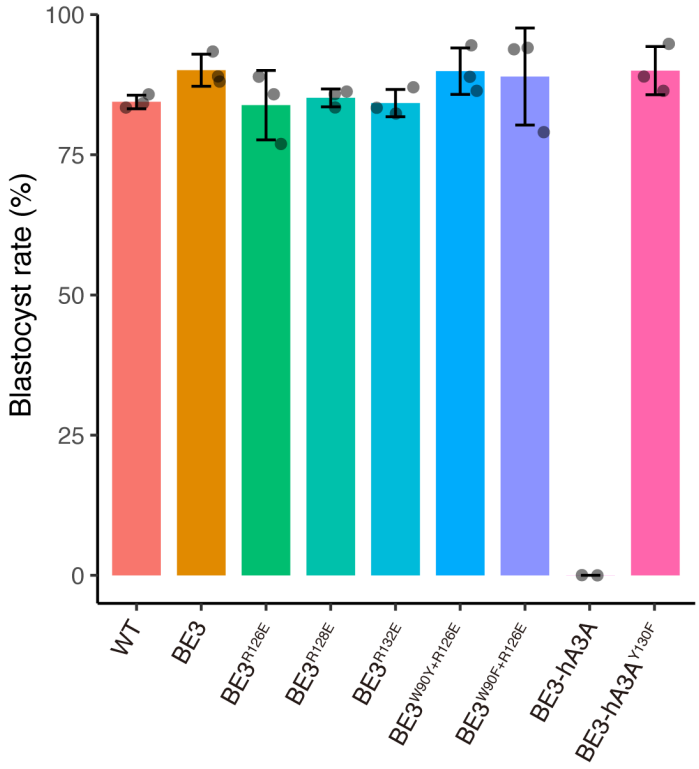

Supplementary Figure 2 The embryonic development rates for BE3 and BE3 variants. *n* = 3 biological replicates for each group.

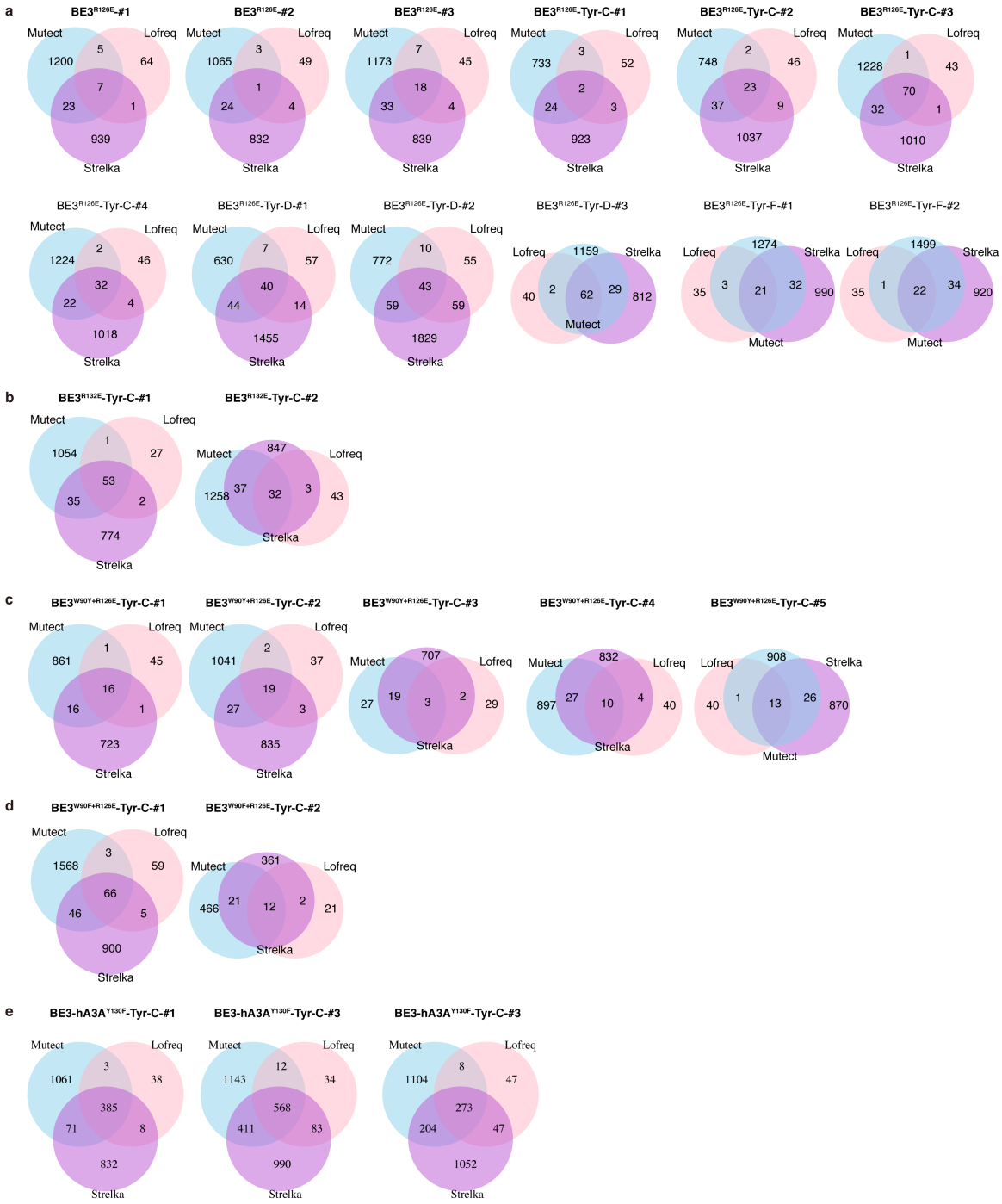

Supplementary Figure 3 Venn diagrams of SNVs detected in each embryo by WGS data using the indicated software tools. a SNVs identified in BE3^{R126E}-treated embryos. **b** SNVs identified in BE3^{R132E}-treated embryos. **c** SNVs identified in BE3$^{W90Y+R126E}$-treated embryos. **d** SNVs identified in BE3$^{W90F+R126E}$-treated embryos. **e** SNVs identified in BE3-hA3A^{Y130F}-treated embryos.

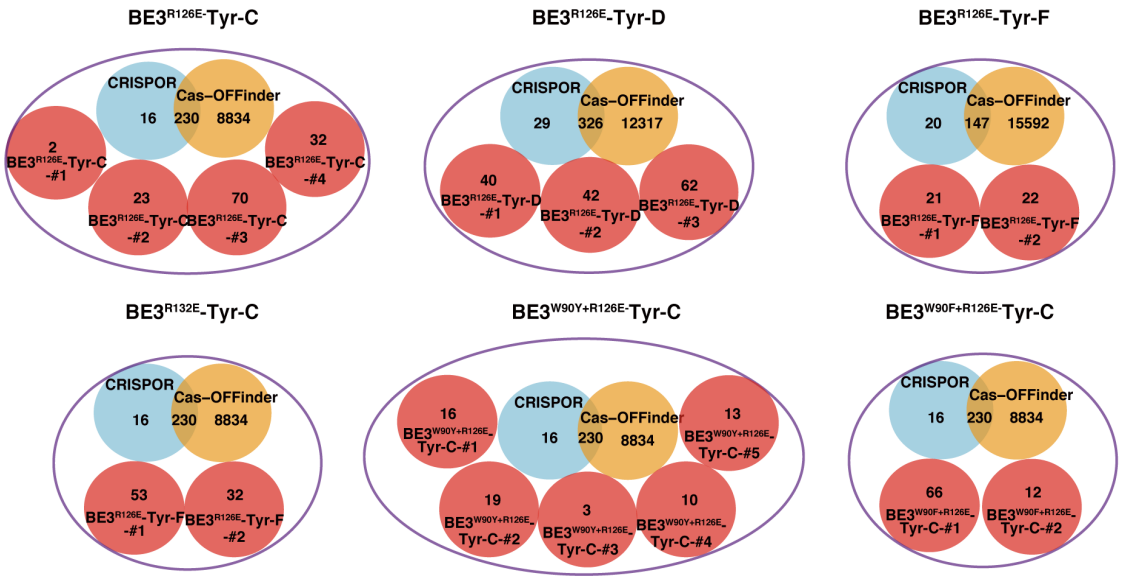

Supplementary Figure 4 The overlap among SNVs detected from our analysis with predicted off-targets sites by Cas-OFFinder and CRISPOR.

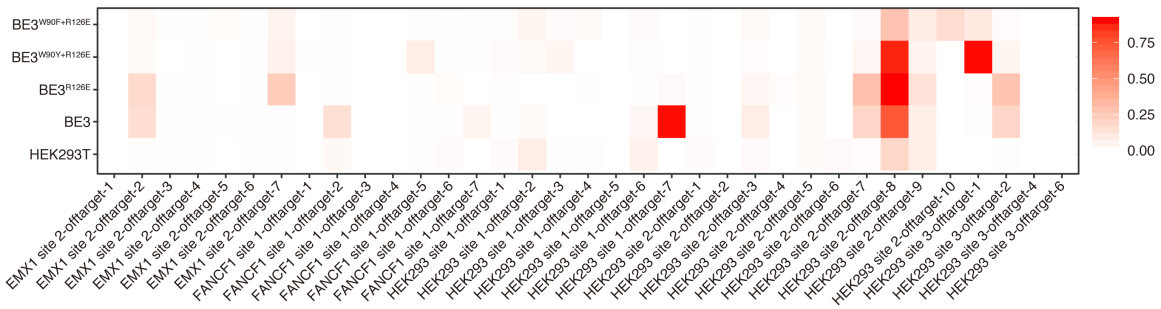

Supplementary Figure 5 Activities of BE3 and BE3 variants at the indicated off-target sites. HEK293T cells were transfected with plasmids expressing BE3, BE3^{R126E}, BE3$^{W90Y+R126E}$ or BE3 $^{W90F+R126E}$ and sgRNAs matching the indicated on-target sequence using Lipofectamine 3000. Three days after transfection, genomic DNA was extracted, amplified by PCR, and analyzed by high-throughput DNA sequencing at the on-target loci, plus the top ten known Cas9 off-target loci for these sgRNAs, as previously determined using the GUIDE-seq method [11, 12] and ChIP-seq method [13]. Sequences of the on-target and off-target protospacers and primers were shown in Table S5. Each cell represents the percentage of total sequencing reads with C to T conversion. $n = 3$ biological replicates for each group.

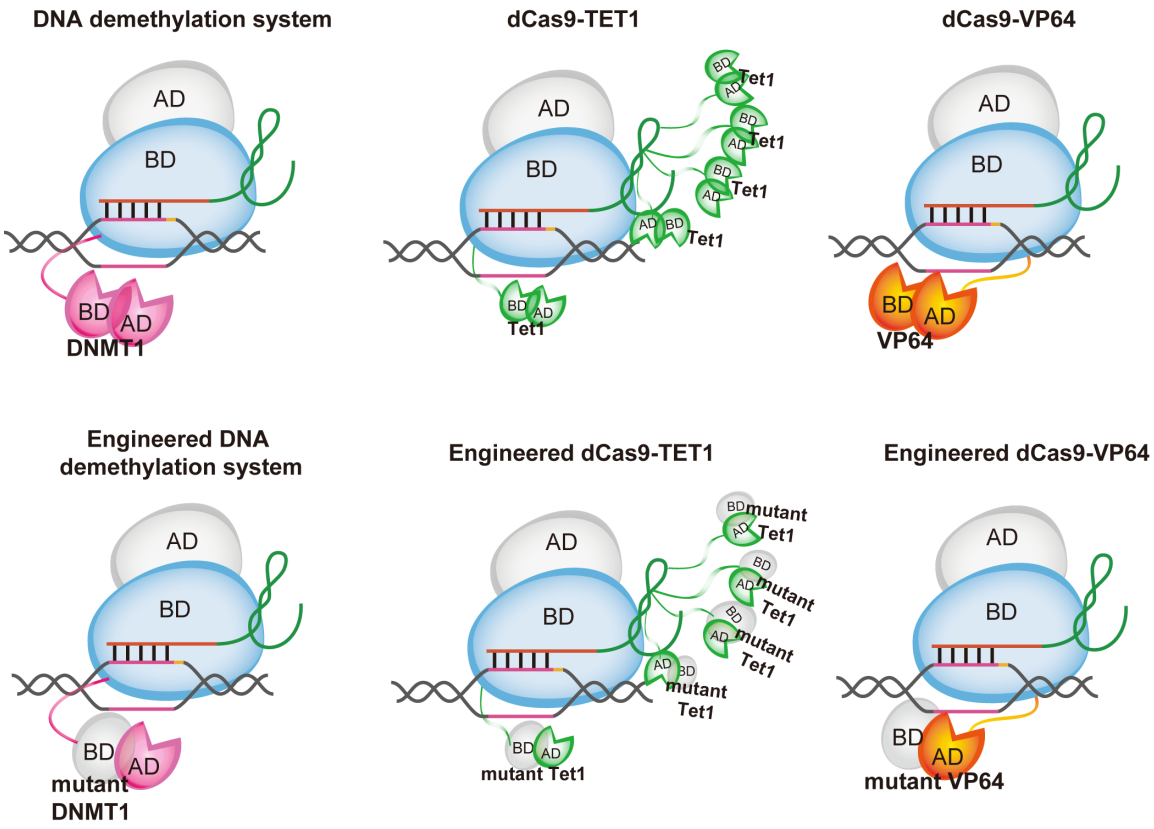

Supplementary Figure 6 The generalization of optimization method for other CRISPR/Cas9 derivates. AD, active domain; BD, binding domain; Tet1, Ten-Eleven Translocation dioxygenase 1.

Supplementary Table 1. P values of the on-target efficiency and indel rates between CBE variants and BE3.

Mutant	On-target efficiency	Indel frequency
Del2-32	0.001	0.046
R33A	0.191	0.957
K34A	0.257	0.605
R33A+K34A	0.748	0.020
Del2-34	0.001	0.032
H61A	0.002	0.014
H61R	0.001	0.015
V62A	0.517	0.724
E63A	0.001	0.015
E63Q	0.001	0.014
Del2-77	0.001	0.017
W90A	0.019	0.411
W90F+R126E	0.095	0.893
W90Y+R126E	0.717	0.126
C93S	0.001	0.016
C96S	0.001	0.018
Del2-116	0.001	0.026
R126E	0.270	0.282
R126E+R132E	0.430	0.027
R126E+R128E+R132E	0.001	0.018
R128E	0.002	0.016
R132E	0.563	0.036
Del169-L	0.001	0.015
Del-182-L	0.001	0.015
P190A+P191A	0.014	0.029
A3A	0.197	0.180
hA3A-Y130F	0.200	0.628

Supplementary Table 2. Summary of HiSeq X Ten sequencing.

Sample	Sample Code	Group	Mapped bases (Gbp)	Coverage
BE3^{R126E}-#1	A21	tdTomato+	120.21	43.38
	A22	tdTomato-	118.12	42.63
BE3^{R126E}-#2	A23	tdTomato+	124.13	44.80
	A24	tdTomato-	121.36	43.80
BE3^{R126E}-#3	A185	tdTomato+	115.12	41.55
	A186	tdTomato-	117.56	42.43
BE3^{R126E}-Tyr-C-#1	A29	tdTomato+	141.77	51.16
	A30	tdTomato-	143.94	51.94
BE3^{R126E}-Tyr-C-#2	A35	tdTomato+	146.12	52.73
	A36	tdTomato-	143.13	51.65
BE3^{R126E}-Tyr-C-#3	A225	tdTomato+	141.81	51.18
	A226	tdTomato-	136.56	49.28
BE3^{R126E}-Tyr-C-#4	A227	tdTomato+	134.54	48.55
	A228	tdTomato-	130.00	46.92
BE3^{R126E}-Tyr-D-#1	A123	tdTomato+	113.09	40.81
	A124	tdTomato-	109.02	39.34
BE3^{R126E}-Tyr-D-#2	A131	tdTomato+	107.61	38.83
	A132	tdTomato-	127.93	46.17
BE3^{R126E}-Tyr-D-#3	A141	tdTomato+	118.05	42.60
	A142	tdTomato-	119.45	43.11
BE3^{R126E}-Tyr-F-#1	A251	tdTomato+	146.49	52.87
	A252	tdTomato-	129.56	46.76
BE3^{R126E}-Tyr-F-#2	A258	tdTomato+	142.19	51.31
	A259	tdTomato-	114.74	41.41
BE3$^{W90Y+R126E}$-Tyr-C-#1	A267	tdTomato+	119.09	42.98
	A268	tdTomato-	142.76	51.52
BE3$^{W90Y+R126E}$-Tyr-C-#2	A269	tdTomato+	142.76	51.52
	A270	tdTomato-	122.23	44.11
BE3$^{W90Y+R126E}$-Tyr-C-#3	A271	tdTomato+	116.99	42.22
	A272	tdTomato-	137.70	49.69
BE3$^{W90Y+R126E}$-Tyr-C-#4	A273	tdTomato+	126.17	45.53
	A274	tdTomato-	148.42	53.56
BE3$^{W90Y+R126E}$-Tyr-C-#5	A275	tdTomato+	130.04	46.93
	A276	tdTomato-	146.61	52.91

BE3$^{W90Y+R126E}$-Tyr-C-#1	A301	tdTomato+	130.76	47.19
	A302	tdTomato-	135.93	49.05
BE3$^{W90Y+R126E}$-Tyr-C-#2	A303	tdTomato+	143.04	51.62
	A304	tdTomato-	149.73	54.04
BE3$^{W90F+R126E}$-Tyr-C-#1	A307	tdTomato+	147.88	53.37
	A308	tdTomato-	117.40	42.37
BE3$^{W90F+R126E}$-Tyr-C-#2	A309	tdTomato+	83.88	30.27
	A310	tdTomato-	126.48	45.64
BE3-hA3A^{Y130F}-Tyr-C-#1	A277	tdTomato+	137.38	49.58
	A278	tdTomato-	152.07	54.88
BE3-hA3A^{Y130F}-Tyr-C-#2	A281	tdTomato+	147.01	53.05
	A282	tdTomato-	149.36	53.90
BE3-hA3A^{Y130F}-Tyr-C-#3	A283	tdTomato+	149.70	54.02
	A284	tdTomato-	151.43	54.65

Supplementary Table 4. Primers used for deep sequencing of on-target activity.

On-target site	On-target sequence	Primer 1	Primer 2
EMX1 site 1	TGCCCCTCCCTCCCTGGCCCAGG	CCAGCTTCTGCCGTTTGTACT	AACTCGTAGAGTCCCATGTCTG
DNMT3B site 2	AGAGCCCCCCCTCAAAGAGAGGG	GATGGCTGTTTGTCTTGTGGC	TATAAACCCTGTGTGCTGCTT
EMX1 site 2	GAGTCCGAGCAGAAGAAGAAGGG	GTTCCAGAACCGGAGGACAA	ATTGCTTGTCCCTCTGTCA
FANCF site 1	GGAATCCCTTCTGCAGCACCTGG	TCCCAGGTGCTGACGTAGGTA	ATCATCTCGCACGTGGTTC
HEK293 site 1	GAACACAAAGCATAGACTGCGGG	GCTAACTGTGACAGCATGTGG	CACCAACTTACACACAGTGA
HEK293 site 2	GGCCCAGACTGAGCACGTGATGG	TTCTGCTTCTCCAGCCCTGGC	TTCATGCAGGTGCTGAAAGCCA
HEK293 site 3	GGCACTGCGGCTGGAGGTGGGGG	CAGAGGGTCCAAAGCAGGAT	TCAACCCGAACGGAGACAC
RNF2 site 1	GTCATCTTAGTCATTACCTGAGG	CGGAACTCAACCATTAAGCA	GTTGCCTTCAAACCTGCTC
EMX1 site 3	GTATTCACCTGAAAGTGTGCAGG	CTTGACTGATATCTCCAGGC	TAGGGGAAGTTGGAGGAGGGAC
PPP1R12C site 1	GGCACTCGGGGGCGAGAGGAGGG	GCTCAAAGTGGTCCGGACTC	TTACCATCCCTCCCTCGACT

Supplementary Table 5. Primers used for deep sequencing of off-target effects.

Site	On-target sequence	Primer 1	Primer 2
EMX1 site 2-On-target	GAGTCCGAGCAGAAGAAGAAGGG		
EMX1 site 2-Off-target-1	GAGTTAGAGCAGAAGAAGAAAGG	TTTCTGAGGGCTGCTACCTG	GCCCCTCTAATACAATGGG
EMX1 site 2-Off-target-2	GAGTCTAAGCAGAAGAAGAAGAG	CTCAATGTGCTTCAACCCATC	ACAGAGCGAGACTCCGTCT
EMX1 site 2-Off-target-3	GAGTCCTAGCAGGAGAAGAAGAG	CAGACTCAGTAAAGCCTGGA	TAGGCTGGAGTGCAGTGGTG
EMX1 site 2-Off-target-4	GAGTCCGGGAAGGAGAAGAAAGG	TCTGCCTCTGACGACGAGCAA	GAGAAAGGCAAACAGGAGG
EMX1 site 2-Off-target-5	AAGTCCGAGGAGAGGAAGAAAGG	TTCATGGAGGGGCACAGAAG	GCCCTTCCAAACTAGAAGTT
EMX1 site 2-Off-target-6	GAATCCAAGCAGGAGAAGAAGGA	GAAACCGAATTATGGATGGG	CTCTTAGAAATGGCATTGGG
EMX1 site 2-Off-target-7	ACGTCTGAGCAGAAGAAGAATGG	TCGTCTTCCTGCAGAGGTTC	ACTCCCATCTTCCTCCCTA
FANCF site 1-On-target	GGAATCCCTTCTGCAGCACCTGG		
FANCF site 1-Off-target-1	GGAACCCCGTCTGCAGCACCAGG	GTCTTAGTCGCCTTAGCACT	ATGTGCTCTGATTTCCGTG
FANCF site 1-Off-target-2	GGAGTCCCTCCTACAGCACCAGG	CATCCCGAACACAGTGACAG	AGATGGAAGAATGAGCAGG
FANCF site 1-Off-target-3	AGAGGCCCCTCTGCAGCACCAGG	AGGACTCAGGCAGGAGTTAG	TGCGGGGTGTGGATGATTT
FANCF site 1-Off-target-4	ACCATCCCTCCTGCAGCACCAGG	TAGAGTGGCATGCAACCTAG	AATGTGCTGGGTCTCTCCT
FANCF site 1-Off-target-5	TGAATCCCATCTCCAGCACCAGG	CAGAAACACTGGAGACCCTC	GATGAAGAAACTGAGGCACA
FANCF site 1-Off-target-6	GGAGTCCCTCCTACAGCACCAGG	CCGAACACAGTGACAGAAGG	GCCCAGTGAGACCAGTTTG

FANCF site 1-Off-target-7	GGAGTCCCTCCTGCAGCACCTGA	GGAAAATTGCTTGTCGCAGC	CCCCTCTGACGGTAATAAT
HEK293 site 1-On-target	GAACACAAAGCATAGACTGCGGG		
HEK293 site 1-Off-target-1	GAACACAATGCATAGATTGCCGG	CATATTTAATGCTCCCACACC	AGCCACATTGTAGACAATGAAGCC
HEK293 site 1-Off-target-2	AAACATAAAGCATAGACTGCAAA	CAGAATAGTGGGACTATGCC	TCACCCTCCTCCTCTCACT
HEK293 site 1-Off-target-3	TCAGGGTGAGCATAGACTGCCGG	AGATAGGACAGGTGAGGCCT	GGCAGGGATGAAAGGTGTC
HEK293 site 1-Off-target-4	TGAAGTGTTGCATAGACTGCAGG	ACCCCTCATGCAAATCCTAAC	TGGGTGGCTAGACTCAGAG
HEK293 site 1-Off-target-5	GGAGAGAGAGCATAGACTGCTGG	TCTGTACCTGCTGGGCATCCA	GAACATCACTCCCATCACG
HEK293 site 1-Off-target-6	CCAAACAAAACATAGACTGCTGG	GGGTAAGACTCTACCCAGGA	TTAATAGCAGTGTGGTGGG
HEK293 site 2-On-target	GGCCCAGACTGAGCACGTGATGG		
HEK293 site 2-Off-target-1	CACCCAGACTGAGCACGTGCTGG	GACAAGAGCATTAACTGCACC	CTCTTCTTCCGAGTGGTGG
HEK293 site 2-Off-target-2	GACACAGACTGGGCACGTGAGGG	GTGGAGTCAGCCTCGATTAC	GATTAGGGTTGCCAAGAGA
HEK293 site 2-Off-target-3	AGCTCAGACTGAGCAAGTGAGGG	TTCAGTCCAGACATCAGCCA	GGCGATGAGTAAGAGTGATGTG
HEK293 site 2-Off-target-4	AGACCAGACTGAGCAAGAGAGGG	actttggaaggtcgaagcggca	TGCATGGTTCATCTCCCCTA
HEK293 site 2-Off-target-5	GAGCCAGAATGAGCACGTGAGGG	GGAAATTGCGAGCAGAGGCT	CTGGGGTCTCTTTCTGCCTC
HEK293 site 2-Off-target-6	CAGGAAGCTGGAGCACGTGAGGG	CATCCCTTGTCTCTCTTAGG	TACACGTTCCACCCCTCCAACC
HEK293 site 2-Off-target-7	AAGGCTGAGGGAGCACGTGAAGG	AGTACAAGCTGATTACATCC	GGTGGAGACAGAAAATGAGG
HEK293 site 2-Off-target-8	GTCAGGGGAAGAGCACGTGACGG	ACTGCAGCCTGGCCCTAAAC	CTACCTCCAAGCCACCAAAC

HEK293 site 2-Off-target-9	GTTGTGAACTGAGCACGTGAGGG	CATTTCCTGTCAGATCACGG	TCAAATGCTCCACCCGCCTCA
HEK293 site 2-Off-target-10	ATATTTGCTGGAGCACGTGAAGG	TCTGAAGCTATGCGCTGGAG	TCAGAACCCCAATACCCCTC
HEK293 site 3-On-target	GGCACTGCGGCTGGAGGTGGGGG		
HEK293 site 3-Off-target-1	TGCACTGCGGCCGGAGGAGGTGG	TGGGCTCACTGCTCTCCAGAGT	AGGAAGGGTACTGGGGAGT
HEK293 site 3-Off-target-2	GGCTCTGCGGCTGGAGGGGGTGG	CAAGTGCTCCCCAATCCTGA	TGGTGAAGAGGATGGGGTGA
HEK293 site 3-Off-target-4	GGCACTGCTACTGGGGGTGGTGG	CCGTTGCTTGTCAGCATCCT	ACTGCTCCCTCTGTTCTCAT
HEK293 site 3-Off-target-6	GGCACTGGGGTTGGAGGTGGGGG	CCATGGCAAACTCTCCACCA	GTCATTTCAGTGGCAGCGGA

References

1. Zuo, E. et al. Cytosine base editor generates substantial off-target single nucleotide variants in mouse embryos. *Science*, published online (2019).
2. Cibulskis, K. et al. Sensitive detection of somatic point mutations in impure and heterogeneous cancer samples. *Nat Biotechnol* **31**, 213-219 (2013).
3. Wilm, A. et al. LoFreq: a sequence-quality aware, ultra-sensitive variant caller for uncovering cell-population heterogeneity from high-throughput sequencing datasets. *Nucleic Acids Res* **40**, 11189-11201 (2012).
4. Saunders, C.T. et al. Strelka: accurate somatic small-variant calling from sequenced tumor-normal sample pairs. *Bioinformatics* **28**, 1811-1817 (2012).
5. Fang, H. et al. Indel variant analysis of short-read sequencing data with Scalpel. *Nat Protoc* **11**, 2529-2548 (2016).
6. Bae, S., Park, J. & Kim, J.S. Cas-OFFinder: a fast and versatile algorithm that searches for potential off-target sites of Cas9 RNA-guided endonucleases. *Bioinformatics* **30**, 1473-1475 (2014).
7. Haeussler, M. et al. Evaluation of off-target and on-target scoring algorithms and integration into the guide RNA selection tool CRISPOR. *Genome Biol* **17**, 148 (2016).
8. Wang, K., Li, M. & Hakonarson, H. ANNOVAR: functional annotation of genetic variants from high-throughput sequencing data. *Nucleic Acids Res* **38**, e164 (2010).
9. Chen, C.C., Hwang, J.K. & Yang, J.M. (PS)2: protein structure prediction server. *Nucleic Acids Res* **34**, W152-157 (2006).
10. Huang, T.T. et al. (PS)2: protein structure prediction server version 3.0. *Nucleic Acids Res* **43**, W338-342 (2015).
11. Tsai, S.Q. et al. GUIDE-seq enables genome-wide profiling of off-target cleavage by CRISPR-Cas nucleases. *Nat Biotechnol* **33**, 187-197 (2015).
12. Komor, A.C., Kim, Y.B., Packer, M.S., Zuris, J.A. & Liu, D.R. Programmable editing of a target base in genomic DNA without double-stranded DNA cleavage. *Nature* **533**, 420-424 (2016).
13. Mali, P. et al. CAS9 transcriptional activators for target specificity screening and paired nickases for cooperative genome engineering. *Nat Biotechnol* **31**, 833-838 (2013).